Improved CO Oxidation via Surface Stabilization of Ceria Nanoparticles Induced by Rare-Earth Metal Dopants

Kyung-Jong Noh,[†] Kyeounghak Kim,[†] Hyung Jun Kim,[†] Dongjae Shin, and Jeong Woo Han[*]

Department of Chemical Engineering, Pohang University of Science and Technology (POSTECH), Pohang, Gyeongbuk 37673, Republic of Korea

Supporting Information

Experimental information

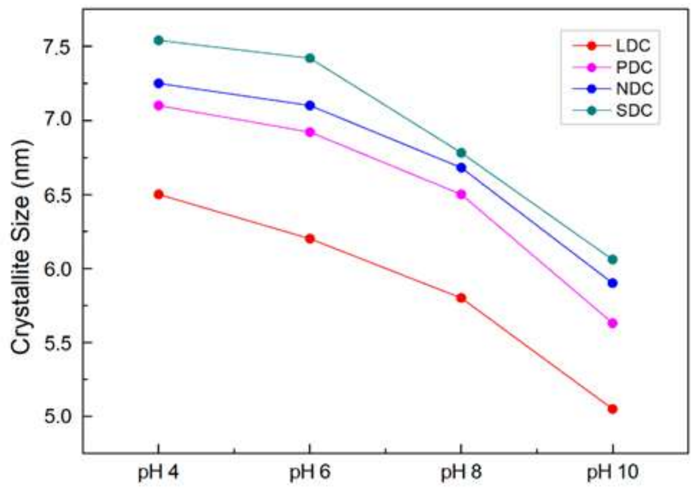

Figure S1: Crystallite size of $Ce_{0.8}RE_{0.2}O_2$ as a function of solution pH (calcined at 500 °C for 3 hours).

Correspondence to jwhan@postech.ac.kr
[†]K.-J. Noh, K. Kim, and H. J. Kim contributed equally to this work.

	$Ce_{0.9}RE_{0.1}O_2$ (RE = 10%)		$Ce_{0.8}RE_{0.2}O_2$ (RE = 20%)	
	Ce (wt%)	RE (wt%)	Ce (wt%)	RE (wt%)
LDC	90.44	9.56	80.67	19.33
PDC	90.67	9.33	81.33	18.67
NDC	91.39	8.61	81.16	18.84
SDC	91.33	8.67	80.92	19.08

Table S1: SEM-Energy Dispersive Spectroscopy (EDS) of well-synthesized composites at the same condition (S-REC); (a) $Ce_{0.9}RE_{0.1}O_2$ and (b) $Ce_{0.8}RE_{0.2}O_2$ nanoparticles.

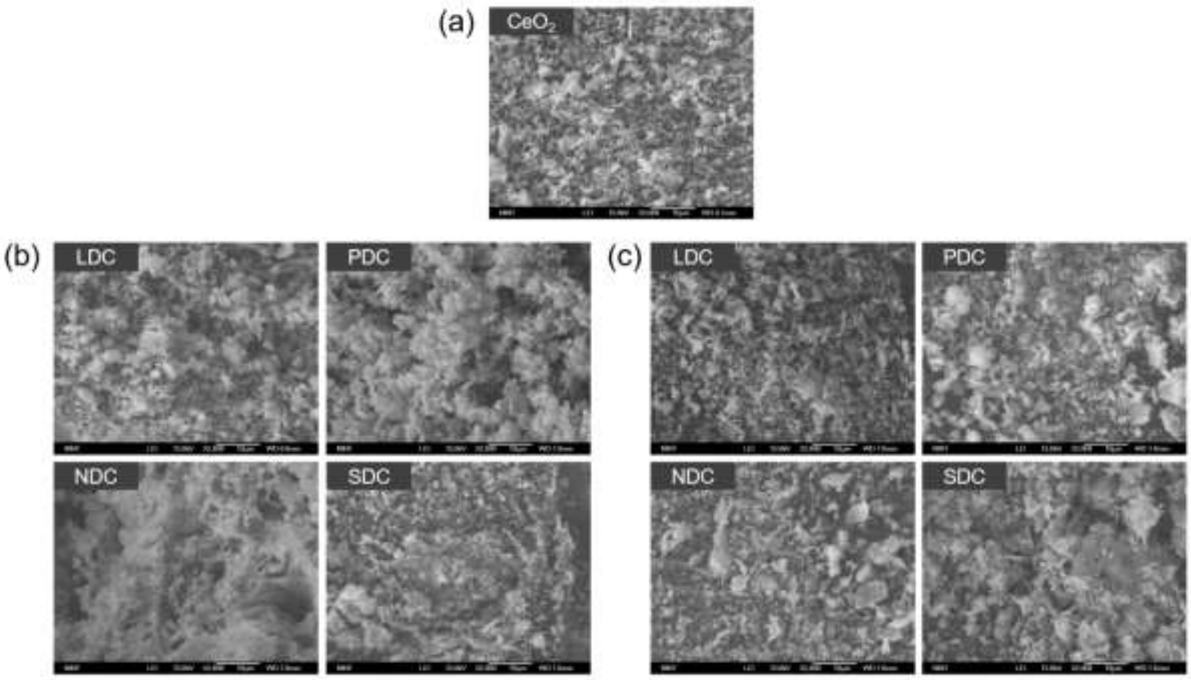

Figure S2: SEM images of well-synthesized composites at the same condition (S-REC); (a) pure CeO_2, (b) $Ce_{0.9}RE_{0.1}O_2$ (RE = 10%), and (c) $Ce_{0.8}RE_{0.2}O_2$ (RE = 20%) nanoparticles.

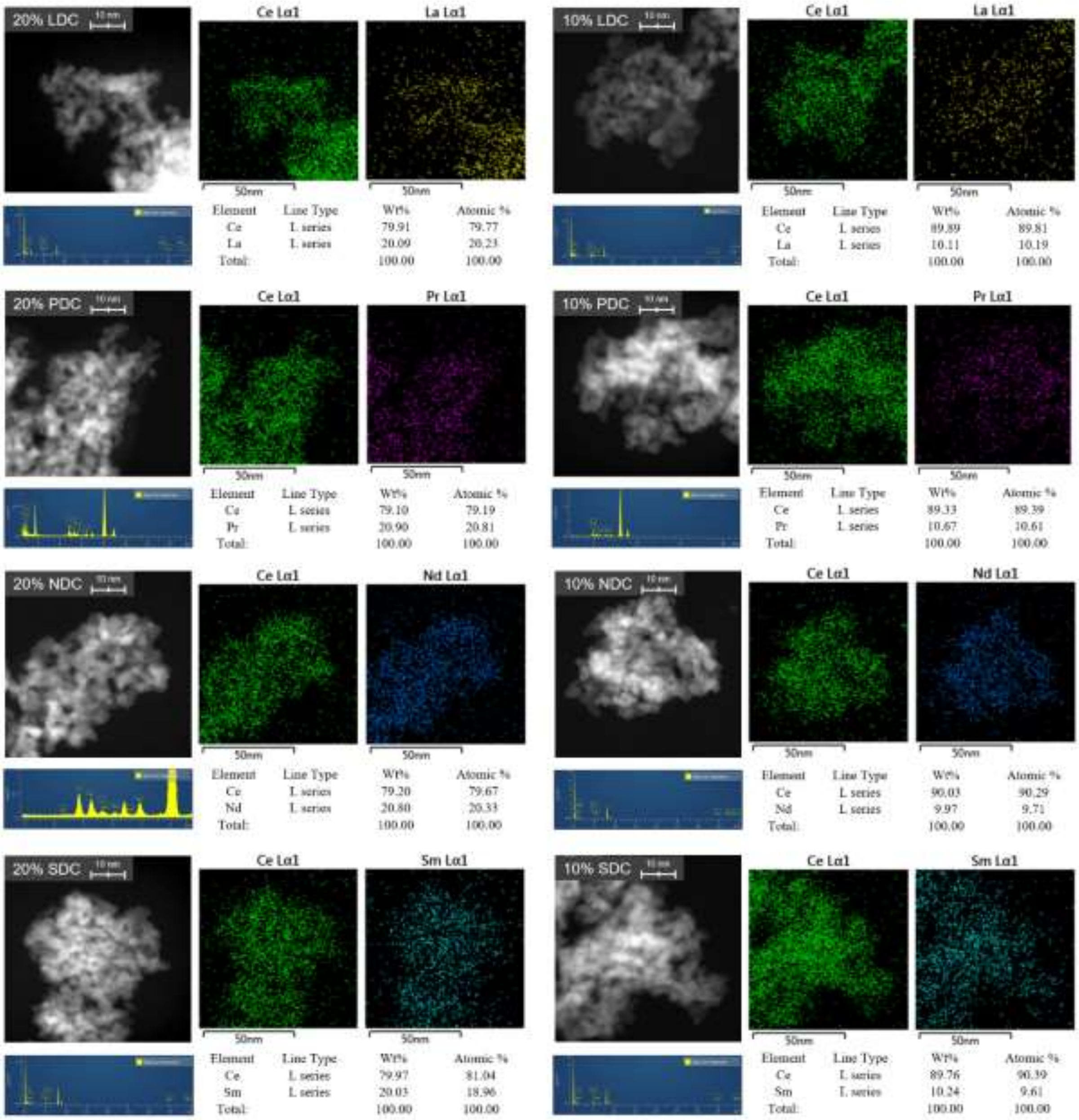

Figure S3: TEM-EDS mapping and distribution analysis of well-synthesized composites at the same condition (S-REC); $Ce_{0.9}RE_{0.1}O_2$ (RE = 10%) and $Ce_{0.8}RE_{0.2}O_2$ (RE = 20%) nanoparticles.

Sample	Ce	RE
20% LDC	$Ce_{0.799}$	$La_{0.201}$
10% LDC	$Ce_{0.899}$	$La_{0.101}$
20% PDC	$Ce_{0.801}$	$Pr_{0.199}$
10% PDC	$Ce_{0.898}$	$Pr_{0.102}$
20% NDC	$Ce_{0.802}$	$Nd_{0.198}$
10% NDC	$Ce_{0.901}$	$Nd_{0.099}$
20% SDC	$Ce_{0.797}$	$Sm_{0.203}$
10% SDC	$Ce_{0.898}$	$Sm_{0.102}$

Table S2: ICP-AES analysis of well-synthesized composites at the same condition (S-REC); $Ce_{0.9}RE_{0.1}O_2$ and $Ce_{0.8}RE_{0.2}O_2$ nanoparticles. The samples were analyzed three times and averaged.

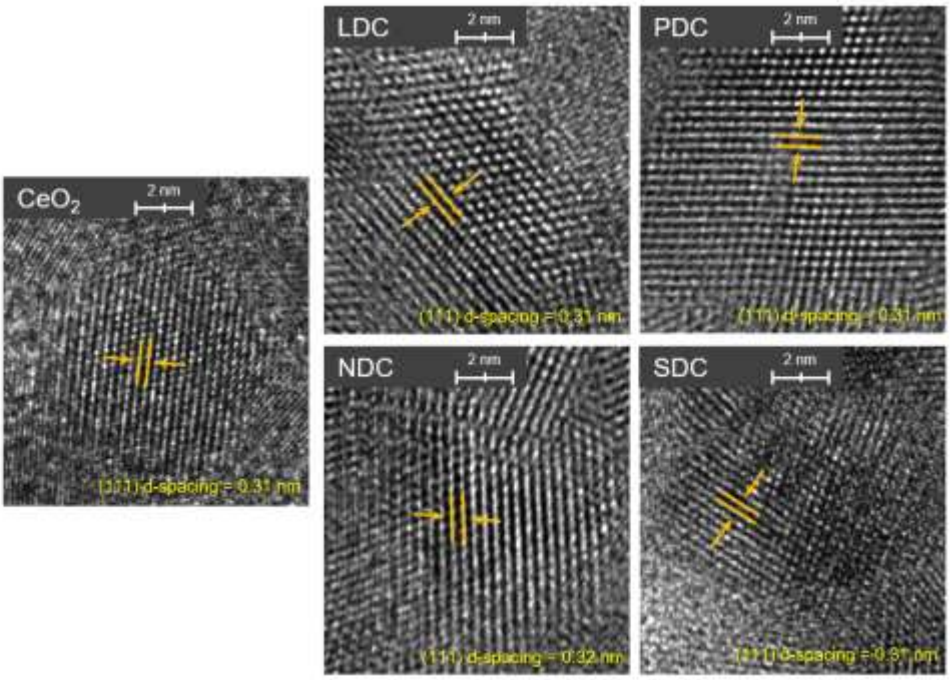

Figure S4: HRTEM images of well-synthesized composites at the same condition (S-REC); pure CeO_2 and $Ce_{0.8}RE_{0.2}O_2$ (RE = 20%) nanoparticles.

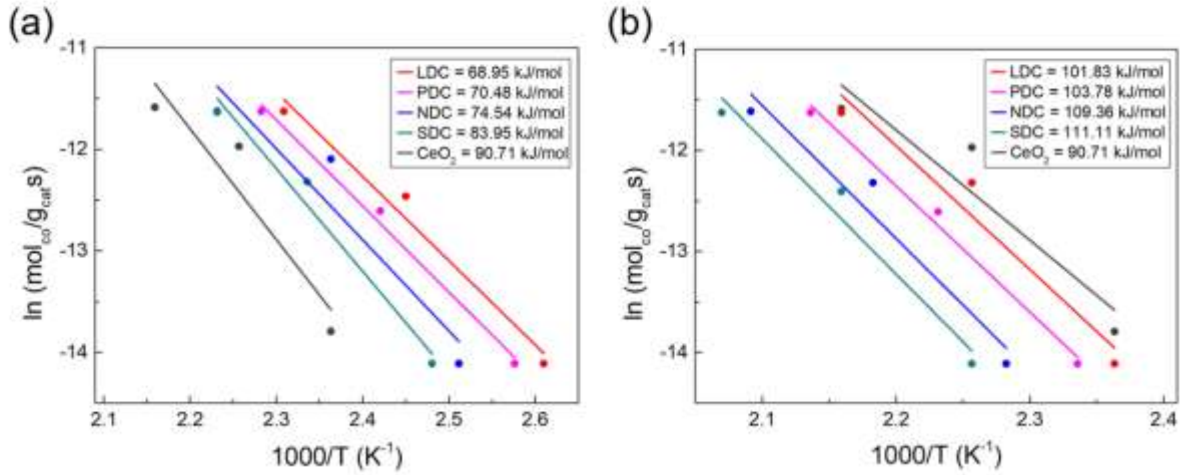

Figure S5: Arrhenius plots for CO oxidation of $Ce_{0.8}RE_{0.2}O_2$ (RE = 20%) composites; (a) S-REC nanoparticles and (b) C-REC nanoparticles.

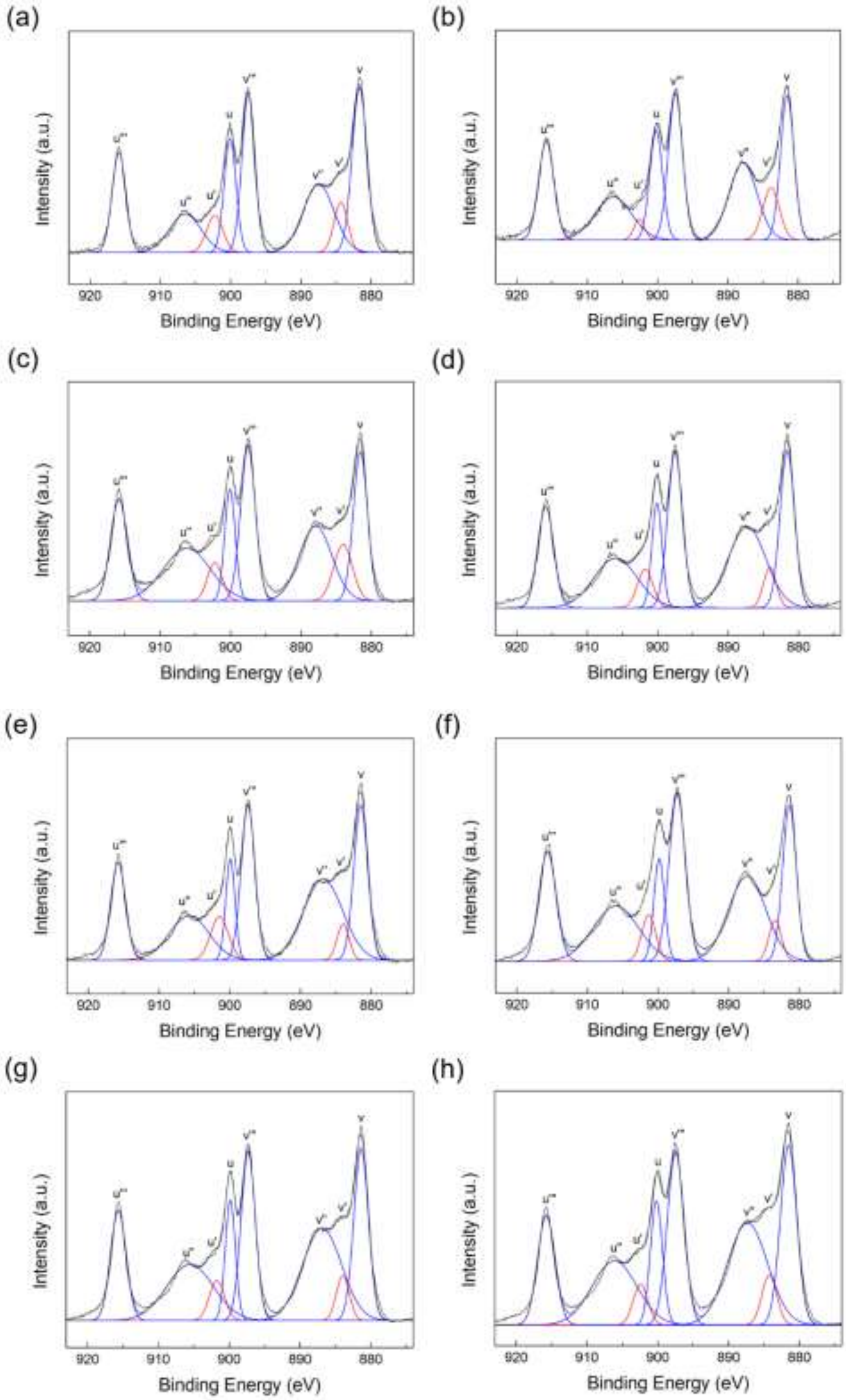

Figure S6: XPS spectra of (a) ~ (d) 20% S-REC nanoparticles; (a) LDC, (b) PDC, (c) NDC, (d) SDC and (e) ~ (h) 20% C-REC nanoparticles; (e) LDC, (f) PDC, (g) NDC, (h) SDC nanoparticles. The peaks of (v'''), (v''), (v), (u'''), (u''), and (u) were assigned to Ce^{4+} species while the peaks of (v') and (u') were assigned to Ce^{3+} species.

Computational information

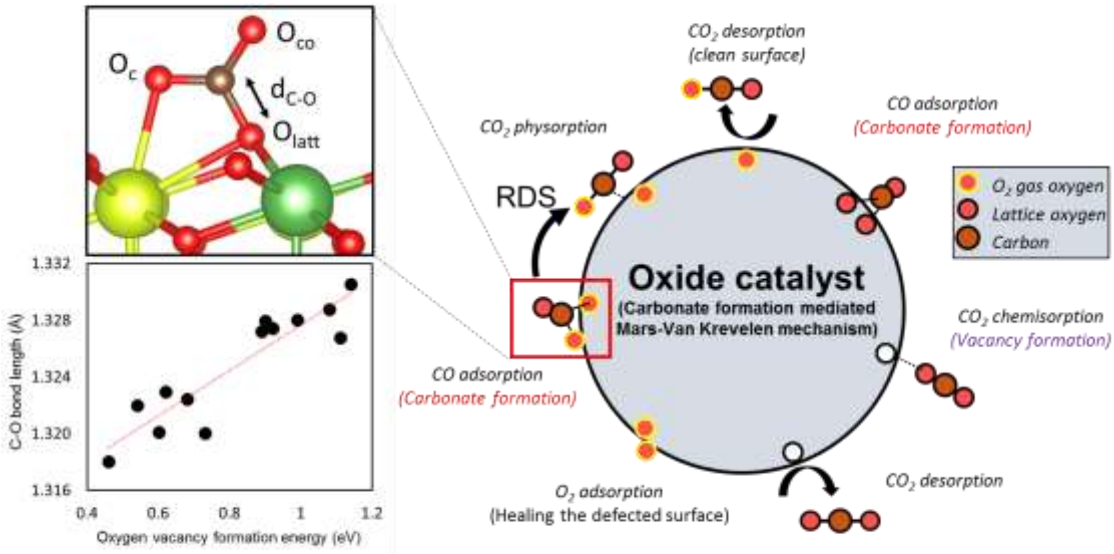

Figure S7: Relationship of bond length between C atom in carbonate species and lattice oxygen (O_{latt}) with oxygen vacancy formation energy of rare earth metal doped CeO_2(111) at rate-determining step of CO oxidation *via* Mars-van Krevelen (MvK) mechanism. Left side of figures are reprinted from Kim et al. with permission.[1] Copyright 2017, Elsevier. Right side of a figure is reprinted from Kim et al. with permission.[2] Copyright 2017, American Chemical Society.

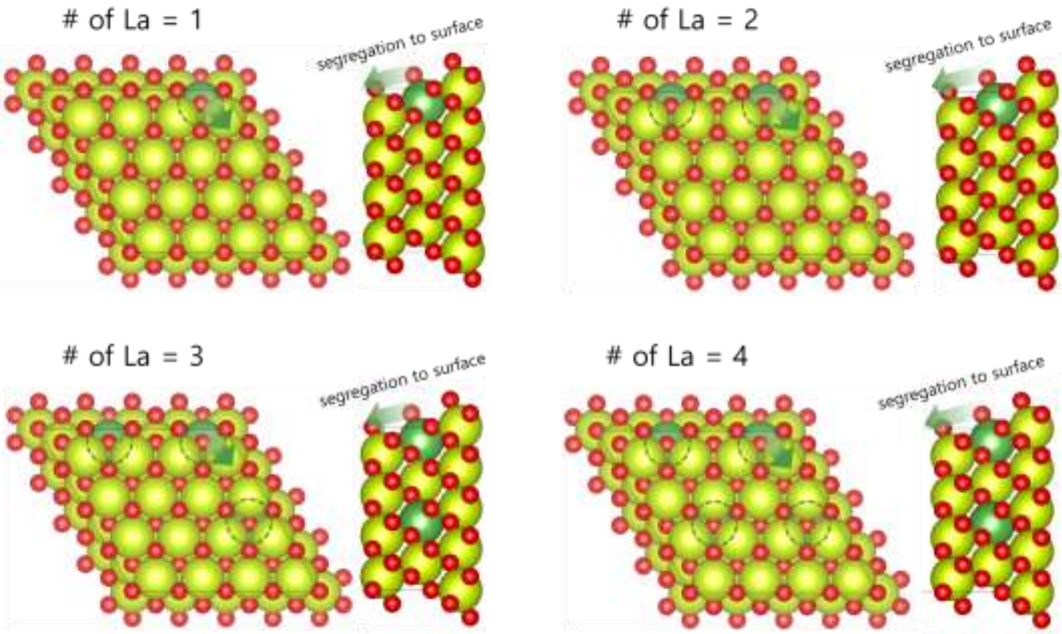

Figure S8. Atomic configurations of La-doped $CeO_2(111)$ (LDC) slab models as a function of the number of La dopants, which were employed to calculate the segregation energies (E_{seg}) of LDCs at different concentrations.

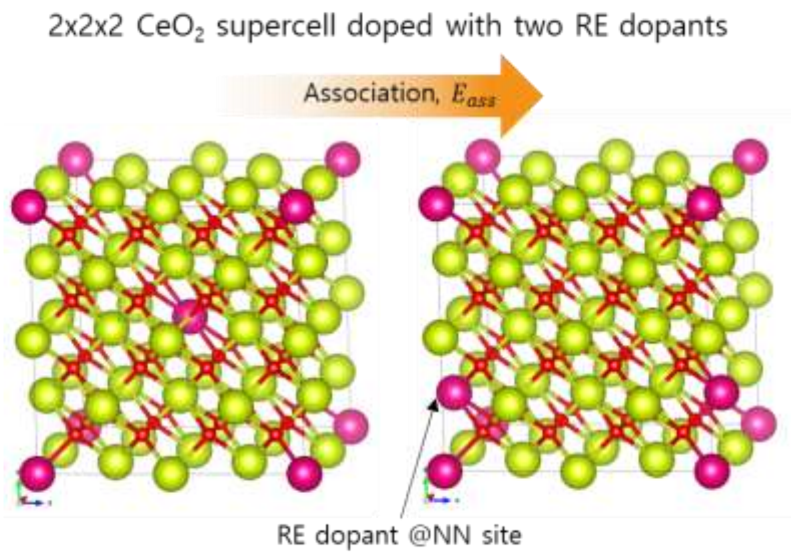

Figure S9. Atomic configurations of RE-doped CeO_2 (REC) bulk models which were employed to calculate the association energies (E_{ass}) of RECs (RE = La, Pr, Nd, Sm).

References

(1) Kim, K.; Yoo, J. D.; Lee, S.; Bae, M.; Bae, J.; Jung, W.; Han, J. W. *ACS Appl. Mater. Inter.* **2017,** *9* (18), 15449-15458.
(2) Kim, K.; Han, J. W. *Catal. Today* **2017,** *293-294,* 82-88.